



High pressure structural behavior of YGa₂: A combined experimental and theoretical study



M. Sekar^{a,*}, N.V. Chandra Shekar^a, R. Babu^b, P. Ch. Sahu^a, A.K. Sinha^c, Anuj Upadhyay^c, M.N. Singh^c, K. Ramesh Babu^d, S. Appalakondaiah^d, G. Vaitheeswaran^d, V. Kanchana^e

^a Materials Science Group, Indira Gandhi Centre for Atomic Research, Kalpakkam-603102, Tamil Nadu, India

^b Chemical Group@, Indira Gandhi Centre for Atomic Research, Kalpakkam-603102, Tamil Nadu, India

^c Indus Synchrotron Utilization Division, Raja Ramanna Center for Advanced Technology, Indore-452013, India

^d Advanced Centre for Research in High Energy Materials, University of Hyderabad, Gachibowli, Hyderabad-500046, Telangana, India

^e Department of Physics, Indian Institute of Technology Hyderabad, Ordnance Factory Estate, Yeddumailaram-502 205, Telangana, India

ARTICLE INFO

Article history:

Received 14 August 2014

Received in revised form

28 January 2015

Accepted 31 January 2015

Available online 9 February 2015

Keywords:

YGa₂

High pressure

X-ray diffraction

Structural transition

ABSTRACT

High pressure structural stability studies were carried out on YGa₂ (AlB₂ type structure at NTP, space group *P6/mmm*) up to a pressure of ~35 GPa using both laboratory based rotating anode and synchrotron X-ray sources. An isostructural transition with reduced *c/a* ratio, was observed at ~6 GPa and above ~17.5 GPa, the compound transformed to orthorhombic structure. Bulk modulus *B*₀ for the parent and high pressure phases were estimated using Birch–Murnaghan and modified Birch–Murnaghan equation of state. Electronic structure calculations based on projector augmented wave method confirms the experimentally observed two high pressure structural transitions. The calculations also reveal that the ‘Ga’ networks remains as two dimensional in the high pressure isostructural phase, whereas the orthorhombic phase involves three dimensional networks of ‘Ga’ atoms interconnected by strong covalent bonds.

© 2015 Elsevier Inc. All rights reserved.

1. Introduction

Rare-earth intermetallic compounds exhibit diversified structural behavior upon the application of hydrostatic pressure [1,2]. For instance, rare-earth digallides undergo structural phase transitions from ambient AlB₂ type structure to orthorhombic (LaGa₂), AlB₂ to AlB₂ with reduced *c/a* ratio (CeGa₂, HoGa₂ and GdGa₂) [3–6]. These structural transitions involve the rearrangements of ‘Ga’ atom networks or with the conservation of ‘Ga’ networks, but with drastic decrease in the *c/a* ratio. In Table 1 the high pressure structures, transition pressures and bulk modulus of different rare-earth digallides REGa₂ (RE=La, Ce, Gd, Ho, Tm, Yb) are shown [7–9]. Yttrium (Z=39), a 4*d* transition metal is often considered as the one belonging to lanthanide series due to several similar physical properties. Yatsenko et al. have studied the phase diagram of Y–Ga system through differential thermal analysis and X-ray diffraction and found that Yttrium digallide YGa₂ crystallizes in the AlB₂ type structure [10].

In the lanthanide series, the structure sequence: hcp→Sm-type→dhcp→fcc→dist. fcc is observed as function of increasing

pressure [11–14]. In La, pressure has the effect of increasing the energy of electrons in the *s*-band relative to the *d*-band, which initiates the *s*→*d* transfer and the number of *d* electrons per atom in the conduction band tends toward 3. A similar electron transfer phenomena has been observed in the non 4*f* element ‘Y’ due to the increased 4*d* band occupancy under high pressure [15,16,7]. Similar structural behavior can be expected in their intermetallic compounds also. In fact, the structural sequence: Cubic (C type)→Monoclinic (B type)→Hexagonal (A type) observed in the lanthanide sesquioxides (Ln₂O₃) as a function of increasing pressure (or decreasing atomic number of the lanthanide element) [17,18]. These considerations encouraged us to investigate the structural modifications of YGa₂ upon the application of pressure. In addition electronic structure calculations based on density functional theory have been carried out to understand the experimentally observed results.

2. Experimental details

YGa₂ was prepared by arc-melting stoichiometric quantities of Y (99.99%) and Ga (99.9%) in helium atmosphere. The arc melted sample was annealed and the powdered sample was characterized by X-ray diffraction (XRD) using a Guinier diffractometer having an

* Corresponding author.

E-mail address: sekarm@igcar.gov.in (M. Sekar).

Table 1

Lanthanide digallides, their high pressure structures, transition pressures and bulk modulus. It may be noted that the c/a ratio for the hexagonal AlB_2 type structure at STP have values ranging from 0.95 to 1.27, whereas that for the high pressure AlB_2 type structure, the values range from 0.59 to 0.88.

Compound	STP structure	High pressure structure	Transition pressure (GPa)	Bulk modulus (GPa)
LaGa ₂	AlB ₂ (hex.)	Orthorhombic	12	166 [7]
CeGa ₂	AlB ₂ (hex.)	AlB ₂ (hex.)	16	72 [4]
GdGa ₂	AlB ₂ (hex.)	AlB ₂ (hex.)	7.7	73,70 [6]
HoGa ₂	AlB ₂ (hex.)	AlB ₂ (hex.)	4	99,103 [5]
TmGa ₂	KH ₂ (ortho.)	AlB ₂ (hex.)	21	95 [8]
YbGa ₂	CaIn ₂ (hex.)	UH ₂ (ortho)	22	20 [5,9]
YGa ₂	AlB ₂ (hex.)	AlB ₂ (hex.)	6	76,112 (this work expt.)
		Ortho	20	119 (this work expt.)

overall resolution of $\Delta d/d \approx 0.0001$. The sample was found to be of good quality, single phase, AlB_2 type (Sp. Group: $P6/mmm$) hexagonal structure with lattice parameters $a = 4.192 \pm 0.001 \text{ \AA}$ and $c = 4.090 \pm 0.090 \text{ \AA}$. Our XRD data on YGa₂ has been accepted as standard PDF file: PDF No: 53-543, ICDD (2002) [19].

High pressure X-ray diffraction (HPXRD) studies on YGa₂ were performed in a Mao-Bell type DAC using angle dispersive X-ray diffraction beamline (BL-12) at INDUS-2 ($\lambda = 0.729 \text{ \AA}$) up to a pressure of ~ 10 GPa. The experiments were also carried out with a laboratory based rotating anode X-ray generator (Rigaku-ULTRAX18) with Mo target ($\lambda = 0.7107 \text{ \AA}$) in conjunction with an image plate based mar345dtb up to a pressure of ~ 35 GPa. The two dimensional X-ray patterns were integrated by using the program FIT2D [20]. Stainless steel (SS) gaskets were preindented to a thickness of $\sim 70 \mu\text{m}$ and a hole of diameter $200 \mu\text{m}$ was drilled at the centre of the compressed area for mounting the sample. A mixture of methanol, ethanol and water (MEW) in the volume ratio 16:3:1 was used as pressure transmitting medium. Both the equation of state of Ag and Ruby fluorescence techniques were used to estimate the sample pressure.

2.1. Computational details

First-principles electronic structure calculations were performed within the framework of density functional theory (DFT) by means of the projector augmented wave (PAW) method as implemented in Vienna Ab-initio Simulations Package [21]. The exchange-correlation potential of Perdew–Burke–Ernzerhof (PBE) for electron–electron interactions is used [22]. To confirm the convergence of the calculations for Brillouin-zone sampling, we have investigated the dependences of the total energy on the cutoff energy and the k -point set mesh according to the Monkhorst–Pack grid scheme [23]. It was found that for the cut-off energy of 800 eV and k -point set of $12 \times 12 \times 8$ the change in total energy is minimum, so we have chosen these for the computation. The self-consistent convergence of the total energy is 1×10^{-8} eV/atom and the maximum force on the atom is 10^{-4} eV/Å.

3. Results and discussion

The HPXRD patterns for YGa₂ at various pressures are depicted in Fig. 1 up to a pressure of ~ 7 GPa using beamline (BL-12) at INDUS-2 synchrotron and in Fig. 2 up to ~ 35 GPa using ULTRAX-18 kW X-ray source. The structure is stable up to a pressure of ~ 6 GPa and all the lines are indexable to the ambient structure. Above ~ 6 GPa, several new peaks start appearing and are

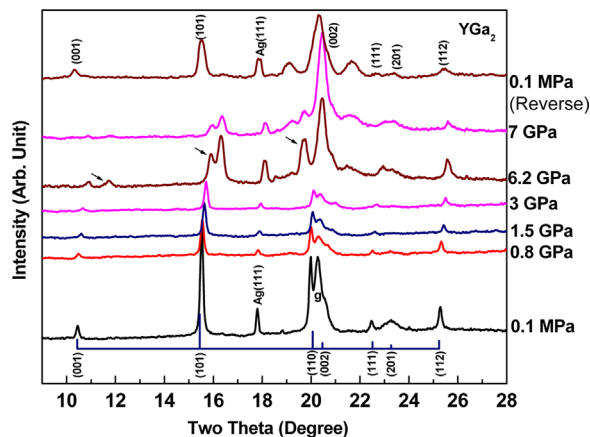


Fig. 1. HPXRD patterns of YGa₂ up to ~ 7 GPa using INDUS-2 synchrotron source with Ag as an internal pressure calibrant ($\lambda = 0.729 \text{ \AA}$). Appearance of new diffraction peaks are indicated by arrows in the 6.2 GPa pattern. The stick plot is the PDF data for YGa₂, and g is the gasket peak.

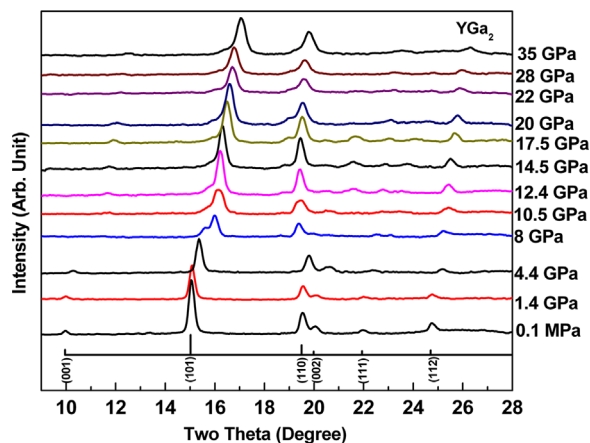


Fig. 2. HPXRD patterns of YGa₂ up to 35 GPa obtained with a RAXRG ($\lambda = 0.7107 \text{ \AA}$). Ruby fluorescence was used to estimate the pressure. The stick plot is the PDF data for YGa₂.

indicated by arrows in Fig. 1. The (1 1 1) peak of Ag was used for pressure calibration in series of experiments summarized in Fig. 1 and ruby fluorescence technique in the series summarized in Fig. 2. A stainless steel (SS) gasket peak was observed at $2\theta = 20^\circ$ overlapping with the (0 0 2) sample peak. The new peaks appeared next to the 100% intensity (1 0 1) peak at $2\theta = 16^\circ$, before the (1 1 0) peak at $2\theta = 19^\circ$ and next to (0 0 1) peak at $2\theta = 12^\circ$. The structural analysis of the high pressure data on YGa₂ was done on trial and error method and various structures were tried. High pressure pattern at ~ 8 GPa with new peaks at 2θ values 11.41, 15.97, 19.39 and 22.58 was considered for analysis. The new phase could be indexed to another AlB_2 type hexagonal crystal structure with lattice parameters: $a = 4.218 \text{ \AA}$, $c = 3.573 \text{ \AA}$, with smaller c/a ratio of 0.84 and good figure of merit. Though it is a mixed phase of both parent and high pressure structures, the new high pressure peaks (0 0 1), (1 0 1), (1 1 0) and (1 1 1) could clearly be indexed up to a pressure of ~ 17.5 GPa. Thus, contrary to the behavior shown by LaGa₂, YGa₂ transforms to another AlB_2 type hexagonal structure with lower c/a ratio. In our earlier experiment on CeGa₂ also, similar type of transition from AlB_2 to another AlB_2 type with reduced c/a ratio at ~ 16 GPa has been observed [4]. Fig. 3 shows the variation of lattice parameters a and c up to ~ 17.5 GPa (experiment) and ~ 18 GPa (computed) for both parent and high pressure hexagonal phases. It is seen that the lattice parameters a and c decreases in both experiment and calculated and around at

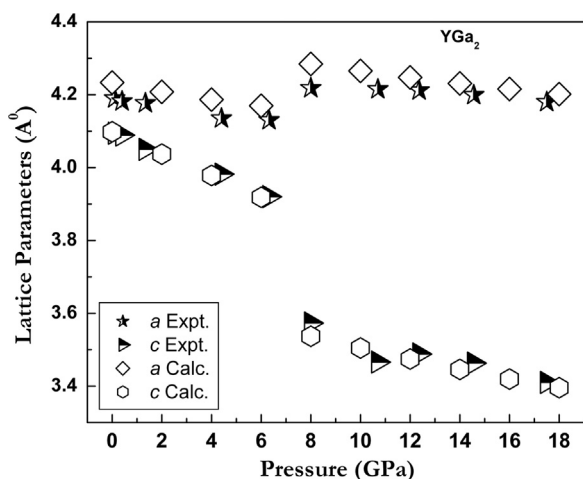


Fig. 3. Variation of lattice parameters a and c of the parent hexagonal phase of $Y\text{Ga}_2$ with respect to pressure up to ~ 17.5 GPa. The computed lattice parameters are also indicated up to 18 GPa.

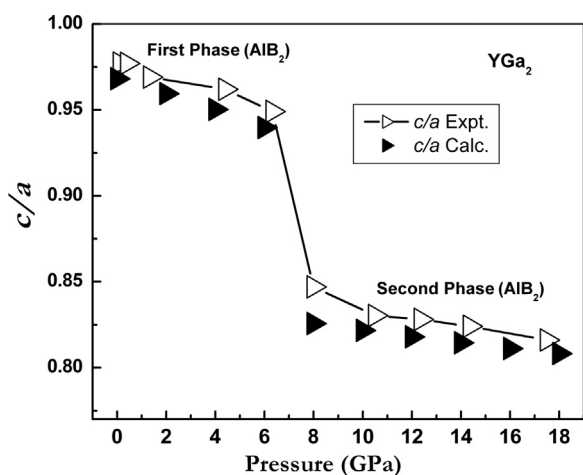


Fig. 4. c/a Ratio of parent and high pressure phase up to ~ 17.5 GPa, along with computed c/a ratio.

~ 8 GPa, a increases to a higher value and decreases systematically with respect to pressure up to a ~ 18 GPa. Whereas, c jumps to a lower value and decreases with increasing pressure. Fig. 4 shows the c/a ratio of the parent and high pressure hexagonal phases as a function of pressure, and a sudden drop in the ratio at ~ 6 GPa is seen. Fig. 5 shows the observed and calculated high pressure XRD patterns of the AlB_2 phase at ~ 8 GPa.

Fig. 6(a) shows the variation of the volume per formula unit for parent and high pressure hexagonal phases. Fig. 6(b) is the P - V data for the parent and HP phases fitted to Birch–Murnaghan and modified Birch–Murnaghan (with subscript P) EOS. The bulk modulus and its derivative for parent and the HP phases are: $B_0 = 76.32 \pm 1$ GPa, $B_0' = 3$, and $B_P = 112 \pm 6.8$ GPa, respectively. The diffraction peaks (1 0 0), (1 0 1), (2 0 0), and (1 0 2) of the high pressure phase could be identified clearly up to ~ 17.5 GPa.

Beyond the pressure of ~ 17.5 GPa, (1 0 1) and (1 1 0) diffraction peaks broadened out significantly and were indexed to orthorhombic structure. Fig. 7 is the variation of the lattice parameters a , b , c of the high pressure orthorhombic phase from 20 to around 35 GPa (40 GPa computed). Fig. 8 is the P - V data of the orthorhombic phase fitted to modified Birch–Murnaghan equation of state. The bulk modulus values are $B_P = 119$ GPa (experimental) $B_P = 125$ GPa (Computed). Table 3 lists all the lattice parameters and volume of every pressure point.

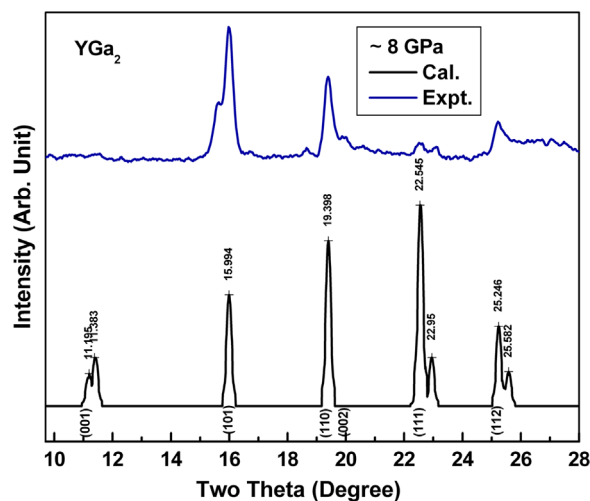


Fig. 5. Observed and calculated patterns of AlB_2 structure at ~ 8 GPa.

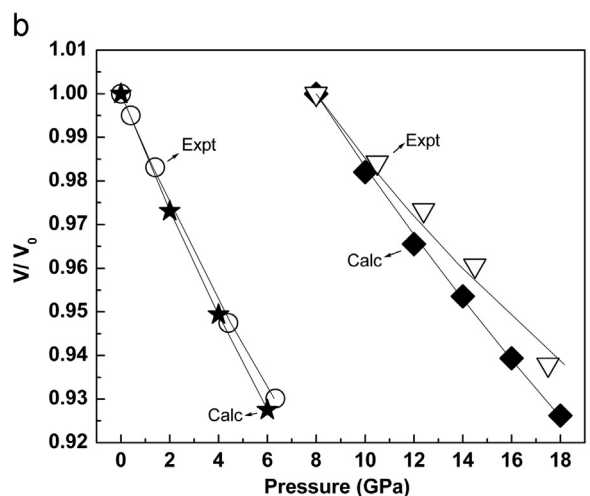
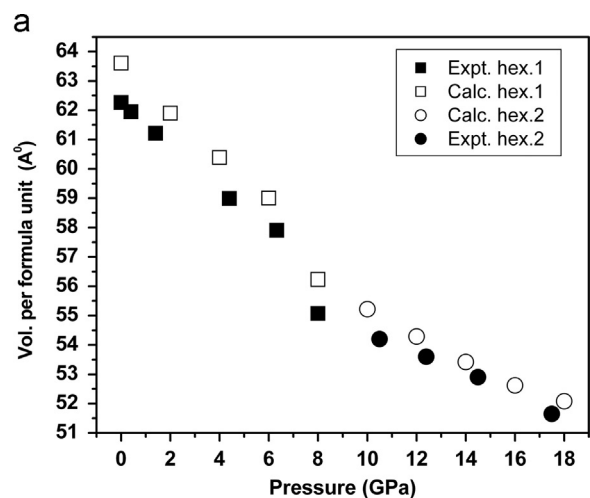


Fig. 6. (a) Shows the variation of the volume per formula unit for parent and high pressure hexagonal phases along with computed values. (b) The P - V data for the parent hexagonal phase of $Y\text{Ga}_2$ up to 6 GPa and new hexagonal phase up to ~ 17.5 GPa. Solid line is the Birch–Murnaghan equation of state fit.

Electronic structure calculations have been carried out to study the structural phase stability of $Y\text{Ga}_2$. As a first step we have optimized the ground state AlB_2 type structure of $Y\text{Ga}_2$ and the corresponding lattice parameters along with experimental data

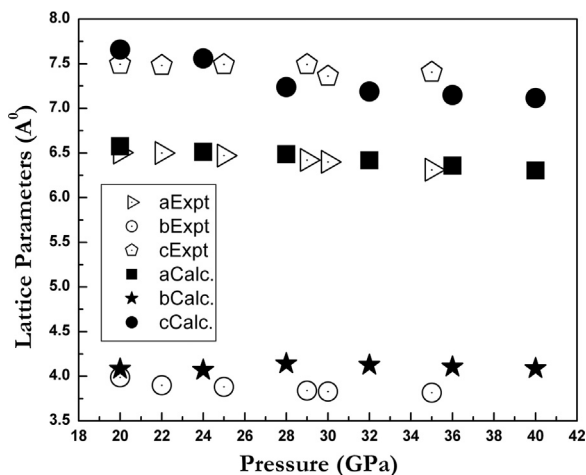


Fig. 7. “a” and “c” for High pressure orthorhombic phase up to 35 GPa (experimental) and 40 GPa (computed).

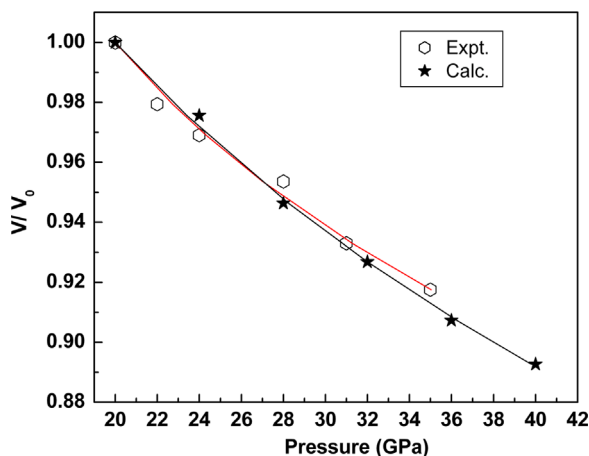


Fig. 8. The P–V data for the orthorhombic phase phase of YGa₂ up to up to 35 GPa (experimental) and 40 GPa (computed).

Table 2

Theoretically obtained structural data of ground state and high-pressure phases of YGa₂. Values in parentheses are from experiment. The present experimental values correspond to the *Imma* structure at 35 GPa.

Pressure (GPa)	Structure type	Space group, z	Lattice parameter (Å)	Volume (Å ³)	Volume/z (Å ³)
0	AlB ₂	<i>P6/mmm</i> , 1	<i>a</i> = 4.233 (<i>a</i> = 4.190) <i>c</i> = 4.098 (<i>c</i> = 4.094)	63.6 (62.26)	63.6 (62.26)
8	AlB ₂	<i>P6/mmm</i> , 1	<i>a</i> = 4.284 (<i>a</i> = 4.218) <i>c</i> = 3.537 (<i>c</i> = 3.573)	56.2 (55.07)	56.2 (55.07)
16	KHg ₂	<i>Imma</i> , 4	<i>a</i> = 6.64 <i>b</i> = 4.10 <i>c</i> = 7.76	211.3	52.8

are tabulated in Table 2. The optimized crystal structure of YGa₂ is shown in Fig. 9(a). The computed lattice parameters are in good accord with experiments with an overestimation of 0.7% to the experimental volume, which is a common feature of GGA based computation for solids. In order to study the structural stability of YGa₂ under pressure, we have applied the pressure in an interval of 2 GPa at each time and allowed the system to relax with respect to cell parameters. At the pressure of 8 GPa, there is a sudden

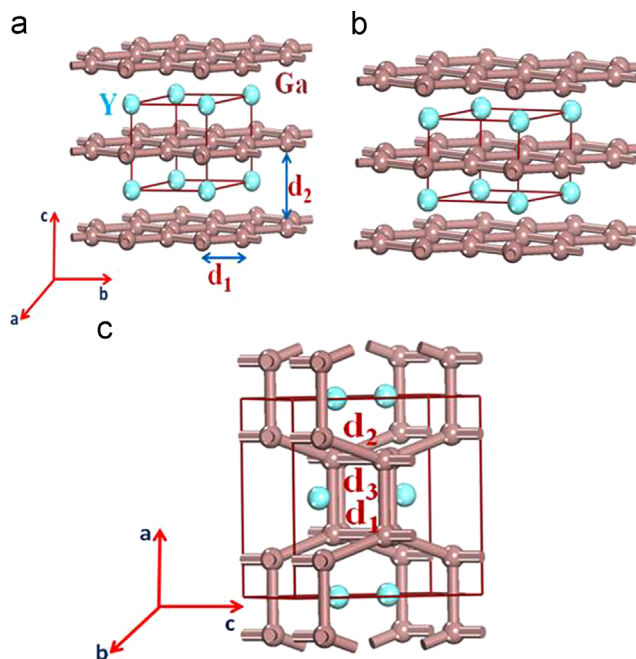


Fig. 9. The optimized crystal structures of YGa₂. (a) Ambient AlB₂ phase (*P6/mmm*), where *d*₁ indicates distance between the ‘Ga’ atoms and *d*₂ indicates distance between the ‘Ga’ layers. (b) High pressure AlB₂ phase. (c) Orthorhombic phase (*Imma*).

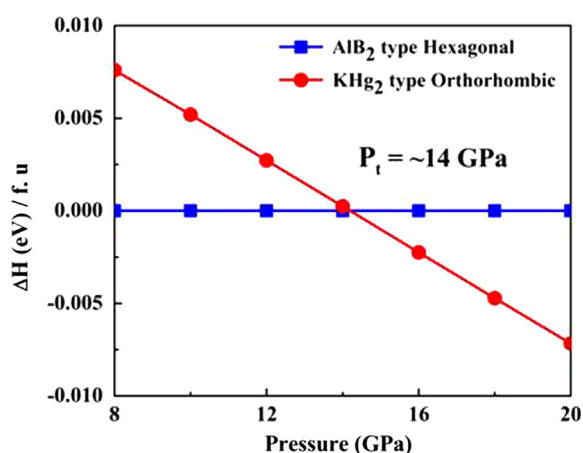
decrease of *c/a* ratio from its initial value 0.97 to 0.82, agreeing with the experimental observations. In Fig. 4, we have shown the calculated variation of *c/a* along with the experimental data. This sudden decrease in the *c/a* ratio confirms that the ambient AlB₂ structure is not stable and undergoes a structural phase transformation to another AlB₂ structure. Earlier, this kind of structural phase transition with pronounced decrease of *c/a* ratio was also observed in the same AlB₂ type compounds HoGa₂ [5] and GdGa₂ [6]. The calculated transition pressure of 8 GPa is in good agreement with the experimental value of 6.2 GPa. In Fig. 8, we have shown the calculated P–V data along with experiment and found that the transition is associated with a volume collapse of 4.6% which is in good accord with experiment. The variation of lattice parameters as a function of pressure is shown in Fig. 3 and they follow similar trend as observed in experiment. Clearly the compression of lattice parameters of YGa₂ is found to be anisotropic in nature. The theoretical bulk modulus and its derivative for parent and the HP phases from Birch–Murnaghan EOS fit results in values of: *B*₀ = 70.53 GPa, *B*₀' = 3.2 and *B*₀ = 111.5 ± 1.2 GPa, *B*₀' = 4.7, respectively.

In order to find the high pressure structural transformation we have computed the enthalpies of both AlB₂ and *Imma* structures and are shown in Fig. 10. At 16 GPa, we could see a structural phase transition and the calculated transition pressure is in good agreement with that of experimental value ~ 17 GPa. Thus, it is indicative that the structural modifications of YGa₂ under high pressure are quite different from that of similar compounds HoGa₂ [5], GdGa₂ [6], and CeGa₂ [4] which undergo only AlB₂ to AlB₂ transition below the pressure of 20 GPa.

The bonding characteristics are useful to understand the structural modifications of YGa₂ at elevated pressures. We have calculated the charge density distribution in YGa₂ by using plane wave pseudopotential method. The calculated charge density of YGa₂ within the (001) plane is shown in Fig. 11. From Fig. 11(a), it is evident that Ga–Ga bond has strong covalent nature in ambient AlB₂ phase which thus causes short distances between ‘Ga’ atoms and it is given by *d*₁(Ga–Ga) = 2.444 Å. In the high pressure AlB₂ phase, the

Table 3
ABC.

Hexagonal (Phase I and II) computed					
P (GPa)	a (Å)	c (Å)	c/a	V (Å ³)	
0.0	4.233 (4.19) ^{Exp}	4.098 (4.094) ^{Exp}	0.9681 (0.977) ^{Exp}	63.61 (62.26) ^{Exp}	
2.0	4.208	4.037	0.9594	61.90	
4.0	4.186	3.979	0.9503	60.39	
6.0	4.170	3.918	0.9397	59.00	
8.0	4.284	3.537	0.8256	56.23	
10.0	4.265	3.505	0.8216	55.22	
12.0	4.248	3.474	0.8179	54.29	
14.0	4.231	3.446	0.8144	53.42	
16.0	4.2156	3.419	0.8111	52.62	
18	4.2016	3.3954	0.8081	51.91	
Hexagonal (Phase I and II) experiment					
P (GPa)	a (Å)	c (Å)	c/a	V (Å ³)	
0.0	4.19	4.094	0.977	62.26	
0.4	4.182	4.089	0.977	61.95	
1.40	4.177	4.05	0.969	61.21	
4.4	4.135	3.982	0.962	58.99	
6.32	4.130	3.92	0.949	57.91	
8	4.218	3.573	0.847	55.07	
10.5	4.215	3.5	0.830	54.20	
12.4	4.212	3.488	0.828	53.60	
14.5	4.199	3.463	0.824	52.90	
17.5	4.18	3.41	0.815	51.65	
Orthorhombic (Phase III) computed					
P (GPa)	a (Å)	b (Å)	c (Å)	V (Å ³)	V (f.u)
20	6.576	4.081	7.657	205.49	51.37
24	6.513	4.069	7.558	200.27	50.07
28	6.485	4.142	7.238	194.43	48.61
32	6.419	4.126	7.188	190.39	47.60
36	6.358	4.106	7.148	186.63	46.66
40	6.304	4.087	7.115	183.28	45.82
Orthorhombic (Phase III) experiment					
P (GPa)	a (Å)	b (Å)	c (Å)	V (Å ³)	V (f.u)
20	6.54	3.92	7.600	194.84	48.71
22	6.463	3.921	7.488	189.794	47.45
24	6.46	3.86	7.483	186.77	46.69
28	6.42	3.840	7.490	185.17	46.29
31	6.40	3.834	7.36	181.03	45.25
35	6.32	3.80	7.40	178.2	44.55

**Fig. 10.** The calculated change in enthalpy as a function of pressure for YGa₂.

covalent bond between Ga–Ga is preserved but with considerable increase in the d_1 value (=2.473 Å) and it is shown in Fig. 11(b). This eventually results in the elongation of lattice parameter 'a' resulting

in low c/a ratio for the high pressure phase and it retains AlB₂ structure with two dimensional layers of 'Ga' atoms because of the similar bonding characteristics. In Fig. 11(c) we have shown the charge density distribution in the high pressure orthorhombic modification of YGa₂. Unlike the AlB₂ structure, it can be clearly seen that 'Ga' atoms form a three dimensional network with increased number of covalent bonds within the unit cell. The distance between the three Ga–Ga bonds d_1 , d_2 , and d_3 are given by 2.4 Å, 2.423 Å, 2.493 Å, respectively. The increase in the number of bonds confirms the structural transition at high pressure.

4. Conclusions

HPXRD studies have been carried out on YGa₂ up to a pressure of ~35 GPa. An iso structural transition with smaller c/a ratio was initiated at ~6 GPa and another transition to orthorhombic phase was initiated at ~17.5 GPa. The orthorhombic structure was stable up to ~35 GPa. The bulk modulus was estimated using the Birch–Murnaghan EOS and its modified form for the high-pressure phase. The electronic structure calculations confirm the experimental findings on structural phase transitions of YGa₂ at high pressures.

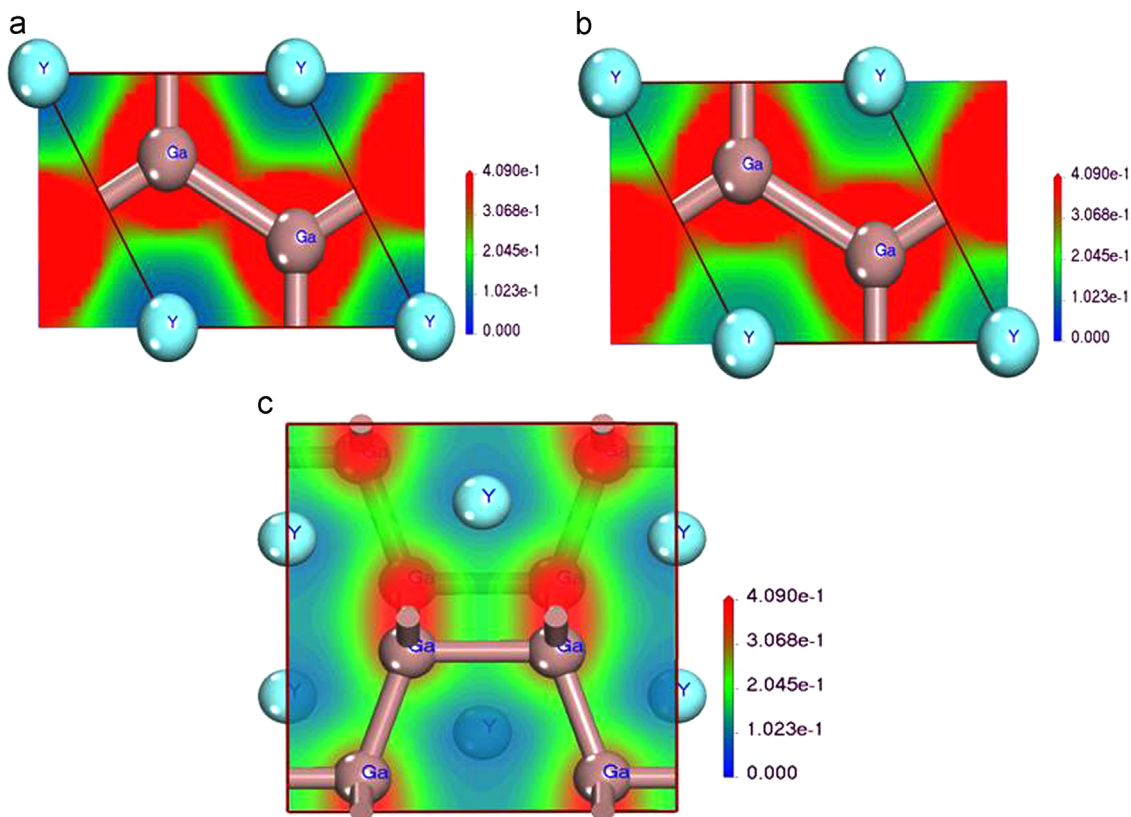


Fig. 11. Charge density distribution along (0 0 1) plane in YGa_2 (a) ambient AlB_2 phase, (b) high pressure AlB_2 phase, (c) Orthorhombic phase.

The calculated transition pressures of 8 GPa and 16 GPa corresponding to AlB_2 and orthorhombic transitions are in good agreement with experiment. The calculations also reveal that the 'Ga' networks remains as two dimensional in the high pressure isostructural phase, whereas the orthorhombic phase involves three dimensional networks of 'Ga' atoms interconnected by strong covalent bonds.

Acknowledgments

The authors thank N.R. Sanjay Kumar, B. Shukla and T.R. Ravindran for valuable discussions. They also thank IGCAR management for their support. G V acknowledges CMSD, University of Hyderabad for providing computational facilities.

References

- [1] R. Demchyna, S. Leoni, H. Rosner, U. Schwarz, Z. Kristallogr. 221 (2006) 420–434.
- [2] M. Sekar, N.V. Chandra Shekar, Sharat Chandra, P. Ch. Sahu, R. Babu, A.K. Sinha, Anuj Upadhyay, M.N. Singh, Philos. Mag. 93 (2013) 4264.
- [3] M. Sekar, N.R. Sanjay Kumar, N.V. Chandra Shekar, D. Sornadurai, P.Ch. Sahu, Philos. Mag. Lett. 91 (2011) 103.
- [4] N.V. Chandra Shekar, N. Subramanian, N.R. Sanjay Kumar, P. Ch. Sahu, Phys. Status Solidi 241 (2004) 2893.
- [5] U. Schwarz, S. Brauning, Yu. Grin, K. Syassen, M. Hanfland, J. Alloys Compd. 268 (1998) 161.
- [6] U. Schwarz, S. Brauning, U. Burhardt, K. Syassen, M. Hanfland, Z. Kristallogr. 216 (2001) 331.
- [7] W.A. Grosshans, Y.K. Vohra, W.B. Holzapfel, J. Magn. Magn. Mater. 29 (1982) 282.
- [8] U. Schwarz, S. Brauning, Yu. Grin, K. Syassen, J. Alloys Compd. 245 (1996) 23.
- [9] U. Schwarz, R. Giedigkeit, R. Niewa, M. Schimdt, W. Schnelle, R. Cardoso, M. Hanfland, Z. Hu, K. Klementiev, Yu. Grin, Z. Anorg. Allg. Chem. 627 (2001) 2249.
- [10] S.P. Yatsenko, A.A. Semyannikov, B.G. Semenov, K.A. Chuntunov, J. Less-Common Met. 64 (1979) 185–199.
- [11] B. Johansson, A. Rosengren, Phys. Rev. B 11 (1975) 2836–2857.
- [12] U. Benedict, W.B. Holzapfel, High pressure studies and structural aspects, in: K.A. Gschneidner Jr, I. Eyring, G.H. Lander, G.R. Choppin (Eds.), Lanthanide and Actinide Physics—I, vol. 17, Elsevier, Amsterdam, 1993 (Handbook on the physics and chemistry of rare-earths).
- [13] W B Holzapfel, J. Alloys Compd. 223 (1995) 170–173.
- [14] J.C. Duthie, D.G. Pettifer, Phys. Rev. Lett. 38 (1977) 564–567.
- [15] G.K. Samudrala, G.M. Tsoi, Y.K. Vohra, J. Phys. Condens. Matter 24 (2012) 362201.
- [16] Y.K. Vohra, H. Olijnik, W.A. Grosshans, W.B. Holzapfel, Phys. Rev. Lett. 47 (1981) 1065.
- [17] I. Halevy, R. Carman, M.L. Winterrose, O. Yeheskel, E. Tifert, S. Ghose, J. Phys. Condens. Matter 215 (2010) 012003.
- [18] P. Ch. Sahu, Dayana Lonappan, N.V. Chandra Shekar, J. Phys. Conf. Ser. 377 (2012) 012015.
- [19] N.V. Chandra Shekar, R. Babu, L.M. Sundaram, I. Kaliappan, P. Ch. Sahu, M. Sekar, K. Nagarajan, K. Govinda Rajan, PDF No: 53-547, ICDD 2002.
- [20] A.P. Hammersley, S.O. Svensson, M. Hanfland, A.N. Fitch, D. Häusermann, High Pressure Res. 14 (1996) 235.
- [21] For Information on VASP, see (<http://www.vasp.at>).
- [22] J.P. Perdew, K. Burke, M. Ernzerhof, Phys. Rev. Lett. 77 (1996) 3865.
- [23] H.J. Monkhorst, J. Pack, Phys. Rev. B 13 (1976) 5188.